

Model-Based Coordinated Control of Four-Wheel Independently Driven Skid Steer Mobile Robot with Wheel/Ground Interaction and Wheel Dynamics

Jianfeng Liao, Zheng Chen, *Senior Member, IEEE* and Bin Yao, *Senior Member, IEEE*

Abstract—Four-wheel independently driven mobile robots are widely used in industrial automation, intelligent inspection and outdoor exploration. The traditional kinematic control is usually applied for them, where only the chassis kinematics is taken into account and the robot dynamics (especially the wheel dynamics) is normally ignored. It may lead to some performance limitations such as the chattering phenomenon during robot rotating, because of the over-actuation characteristic by four driving wheels. To address these problems, the integrated dynamic model is proposed, which includes chassis kinematics, chassis dynamics, wheel/ground interaction, and wheel dynamics. Subsequently, different from kinematic control, a model-based coordinated adaptive robust controller is developed, which generally consists of three-level designs for different parts of robot dynamics, and directly generates the motor driving torque commands for four wheels. The stability and tracking performance are theoretically guaranteed. Comparative experiments are carried out, and the results show the better performance of our proposed scheme.

Index Terms—Coordinated control, mobile robot, adaptive control, robust control, control allocation.

I. INTRODUCTION

With the improvement of robot performance, the range of application of mobile robots has been greatly expanded. It has not only been widely used in industries, agriculture, medical care and service but also applied in dangerous places such as national defense and outdoor exploration [1], [2]. Among them, the skid-steer type mobile robots are usually used in outdoor explorations due to its simple mechanical structure and better rough terrain adaptation ability as shown in Fig.1. Generally, the skid-steer mobile robot is equipped with four independent driving motors to increase the driving ability based on the practical requirements.

The tracking control of the mobile robot has drawn a significant attention from research institutes and industries, and is an important research topic. In the present, a great deal of work has been investigated on the dynamic modeling and controller design of mobile robots [3], [4], [5], [6]. However,

This work is supported by National Natural Science Foundation of China (No.61603332, No.51875508 and No.U1609211), Science Fund for Creative Research Groups of National Natural Science Foundation of China (No.51521064). (*Corresponding author: Zheng Chen*).

Jianfeng Liao, Zheng Chen and Bin Yao are with the State Key Laboratory of Fluid Power and Mechatronic Systems, Zhejiang University, Hangzhou 310027, China (e-mail: jfliao91@foxmail.com, cwlinus@gmail.com, byao@zju.edu.cn). Zheng Chen is also with the Ocean College, Zhejiang University, Hangzhou 310027, China (e-mail: zheng_chen@zju.edu.cn). Bin Yao is also with the School of Mechanical Engineering, Purdue University, West Lafayette, IN 47907 USA (e-mail: byao@purdue.edu).

most of them focused on two-wheel driven or car-like robots, and seldom researches pay attention to the control of four-wheel independently driven mobile robots. Among them, the kinematic model based control law is the most widely used in actual application[7], [8] due to its simple controller design. This kind of controller is developed to directly generate the reference wheel velocities based on the approximate relations between wheels and the robot. With the kinematic controller, the performance will also be limited due to the ignore of dynamic model. Thus, to improve the tracking performance, several control methods have been proposed by considering the robot's dynamics [5], [9]. In the present work, most control methods are proposed with dynamic model of two-wheel mobile robots. Some researches also developed the controller for mobile robot with four driven wheels [10], [11]. However, since the driving wheels are mechanically connected together on same side, the proposed control scheme is similar with the two-wheel driven type and the over-actuated driving problem is still remained unsolved. Compared with the above two-wheel driven mobile robot, the over-actuated feature can not be ignored for the control of the mobile robot with four independently driven wheels. To address the over-actuated problem, the control allocation becomes a possible approach. Some control allocation methods are developed for over-actuated electrical vehicle [12], [13], where the controller are developed with direct driving torque distribution based on specified cost function. Different from the electrical vehicle, the suspension system and steer system are lacked for most mobile robot. Thus, the controller for the vehicle can not be simply applied for the four-wheel mobile robot. In [14], a torque allocation control with a feedback compensation to limit wheel velocity is proposed, which provides a simplified control solution for the over-actuation characteristic of four-wheel mobile robot. But the wheel/ground interactions and wheel dynamics are not taken into account yet, which may lead to some limitations since these parts of dynamics are important and the practical control inputs are the motor driving torques of four wheels.

To take the wheel dynamics into control design, a mathematic model for the wheel dynamics and the complex interactions between the wheels and ground is needed. So far, there are already some researches about the modeling of the wheel/ground interactions for mobile robots [1], [15]. Some researches also developed the controller with consideration of the wheel slips [4], [5], [16]. However, the above studies focus on the controller design with slip compensation and

complex wheel/ground interactions are usually ignored. Thus, the partial work in this paper is to present a dynamic model of the robot with four independent driven wheels, which includes the over-actuated feature, coupled wheel/ground interactions and wheel dynamics. On the other side, the model based control of mobile robot by directly considering the complex dynamics becomes another challenging issue. Recently, lots of model based control laws have been developed, such as adaptive control [17], [18], [19], [20], [21], optimization method [22], [23], [24], [25] and robust control [26], [27], [28], [29], for different mechanical systems as the linear motor [30], [31], [32], robots [33], [34] and hydraulic system [18]. In addition, the adaptive robust controller has been widely applied in different industrial fields and verified with experimental results [35], [36], [37], where the tracking accuracy is guaranteed in general while achieving good robustness in the absence of unstructured uncertainties. These controllers could be applied for the dynamic control synthesis of mobile robots. Furthermore, an appropriate control strategies are also needed to handle the over-actuated problem, wheel/ground interactions and wheel dynamics for the mobile robot with four independent wheels in this paper.

In this paper, a model-based coordinated adaptive robust control scheme is proposed for four-wheel independently driven skid steer mobile robot. Different from the kinematic control, the proposed dynamic controller directly generates the motor driving torque commands for four wheels with consideration of the over-actuated problem, wheel/ground interactions and wheel dynamics, and generally consists of three-level subsystems. In the high level of the proposed controller, by mainly focusing on the chassis dynamics, an adaptive robust control law [35], [38] is proposed to track the desired robot motion trajectory and generates virtual friction driving force for the later middle level control design. In the middle level, to deal with the over-actuated feature, a control allocation method [39], [40], [41] considering the wheel/ground interactions is proposed such that the wheel slip reference is generated for each wheel in the low-level design. And in the low level, the adaptive robust wheel slip control is designed to track the desired wheel slip reference with consideration of the wheel dynamics. Theoretically, the stability of the proposed controller is guaranteed and the tracking performance can be improved.

The rest of this paper is organized as follows. In Section II, we present a kinematic and dynamic model with over-actuated feature, wheel/ground interactions and wheel dynamics for a four-wheel independently driven mobile robot. In section III, a three-level adaptive robust trajectory tracking controller integrated with control allocation technique is proposed. Experiments on a mobile robot are carried out and the results are compared in section IV. Finally, we present the conclusion in section V.

II. SYSTEM MODELING AND PROBLEM FORMULATION

In this section, the kinematic and dynamic model of a four-wheel independently driven mobile robot is derived for controller design, which contains high level robot chassis model, low level wheel model and wheel/ground interactions.

A. System modeling

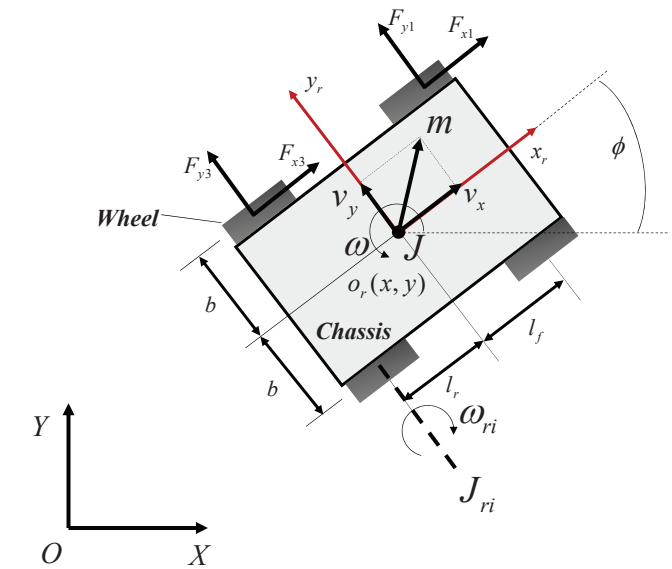


Fig. 1. Top view of a four-wheel independently driven mobile robot

Let $O - XY$ be the reference coordinate system and $o_r - x_r y_r$ be the coordinate system attached on the mobile robot as shown in Fig.1. The width between the driving wheels is represented as $2b$. The distances from the gravity center to the front and rear wheel axles are l_f and l_r respectively. In this figure, m represents the mass of mobile robot; J is the inertia of mobile robot; J_{ri} denotes the inertia of driving wheel; F_{xi} and F_{yi} represent the longitudinal and lateral wheel/ground interactions respectively. (x, y) and ϕ are the position and orientation of the mobile robot with respect to the reference coordinate frame respectively. v_x , v_y and ω denote the longitudinal, lateral and angular velocity of the mobile robot chassis. ω_{ri} is the angular velocity of the driving wheel. From the figure, we can find that the model consists of three parts: the mobile robot chassis dynamics(to describe the motion of mobile robot chassis), the driving wheel dynamics(to describe the motion of driving wheel) and the wheel/ground interactions(the relationship between the motion of mobile robot chassis and driving wheel).

The kinematic model of mobile robot chassis is given as[1]

$$\dot{\mathbf{q}} = \begin{bmatrix} \cos(\phi) & 0 \\ \sin(\phi) & 0 \\ 0 & 1 \end{bmatrix} \mathbf{v} + \begin{bmatrix} -\sin(\phi) \\ \cos(\phi) \\ 0 \end{bmatrix} v_y \quad (1)$$

where $\mathbf{q} = (x, y, \phi)^T$ and $\mathbf{v} = [v_x, \omega]^T$. As seen from Fig.1, we can obtain the dynamic model of the mobile robot chassis

$$\begin{aligned} m(\dot{v}_x - v_y \omega) &= u_x + d_x \\ m(\dot{v}_y + v_x \omega) &= u_y + d_y \\ J\dot{\omega} &= u_\phi + d_\phi \end{aligned} \quad (2)$$

where $u_x = \sum_{i=1}^4 F_{xi}$ is defined as the combined longitudinal driving force on the mobile robot; $u_y = \sum_{i=1}^4 F_{yi}$ is the sum of lateral friction forces; $u_\phi = -bF_{x1} + l_f F_{y1} + bF_{x2} + l_f F_{y2} - bF_{x3} - l_r F_{y3} + bF_{x4} - l_r F_{y4}$ denotes the combined

yaw torque resulted from the frictions; d_x, d_y , and d_ϕ represent disturbances. Thus, the dynamic model(2) can be derived as

$$\begin{aligned} \mathbf{M}\dot{\mathbf{v}} + \mathbf{B}v_y &= \mathbf{u} + \mathbf{d} \\ m(\dot{v}_y + v_x\omega) &= u_y + d_y \end{aligned} \quad (3)$$

where $\mathbf{M} = diag[m, J]$ denotes the inertia matrix; \mathbf{B} is matrix written as $[-m\omega, 0]^T$; $\mathbf{u} = [u_x, u_\phi]^T$ denotes the driving force and yaw moment vector; $\mathbf{d} = [d_x, d_\phi]^T$ is the lumped disturbance and modeling uncertainty. The second term in equation(3) describes the lateral slip motion.

From the equation(2), the motion of the mobile robot is resulted from the wheel/ground interactions F_{xi} and F_{yi} , that mainly consists of friction forces. For the traditional two-wheel mobile robot, the wheel/ground interactions are usually ignored in the dynamic model due to the pure rolling assumption. However, since the special mechanical structure of the four-wheel independently driven mobile robot, the pure rolling assumption is not hold, and the traditional model is not suitable for controller design. In contrast, the wheel/ground interactions are considered in this paper, and a great deal of friction models have been proposed to describe the wheel/ground interactions[34] (e.g. Lugre model, Dugoff's model). Most of them are so complex that are not necessary for controller design. Thus, an appropriate friction model similar with approach[1] is applied, where the relation between frictions and wheel slip is shown in Fig.2. And the friction

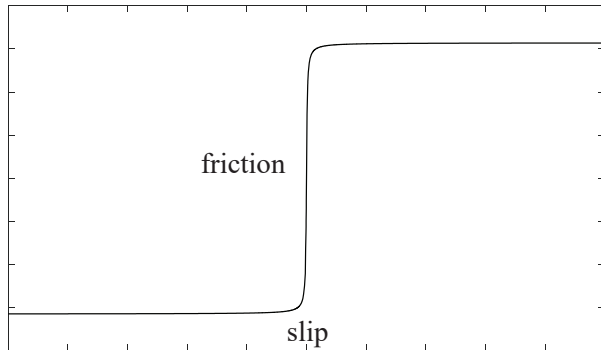


Fig. 2. An appropriate friction model

force can be calculated as

$$\begin{aligned} F_{xi} &= N_i \mu_f S_f(s_i) \frac{s_{xi}}{s_i}, F_{yi} = N_i \mu_f S_f(s_i) \frac{s_{yi}}{s_i} \\ s_i &= \sqrt{s_{xi}^2 + s_{yi}^2} \end{aligned} \quad (4)$$

where N_i represents the vertical force of each wheel; μ_f is the friction coefficient; the dynamic feature of the friction force can be approximated by $S_f(s_i) = 2/\pi \operatorname{atan}(90s_i)$; s_{xi} and s_{yi} represent the longitudinal and lateral slip, which are defined as

$$\begin{aligned} s_{x1} &= r\omega_{r1} - v_x + b\omega, s_{y1} = v_y + l_f\omega \\ s_{x2} &= r\omega_{r2} - v_x - b\omega, s_{y2} = v_y + l_f\omega \\ s_{x3} &= r\omega_{r3} - v_x + b\omega, s_{y3} = v_y - l_r\omega \\ s_{x4} &= r\omega_{r4} - v_x - b\omega, s_{y4} = v_y - l_r\omega \end{aligned} \quad (5)$$

From Fig.3, the rotational dynamics of each driving wheel can derived as

$$J_{ri}\ddot{\omega}_{ri} + c_{ri}\omega_{ri} + f_{ri} = u_{ri} - rF_{xi} + d_{ri}, i = 1, 2, 3, 4 \quad (6)$$

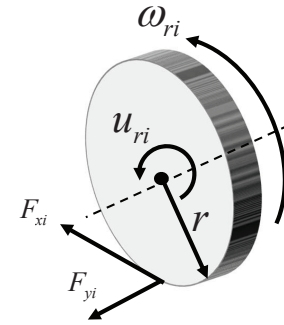


Fig. 3. Wheel rotational motion

where the damping coefficient is represented as c_{ri} ; the Coulomb's friction of the rotation shaft $f_{ri}(\omega_{ri})$ is approximated by $f_{ri} = A_{fi}S_f(\omega_{ri})$; u_{ri} is the motor input torque; d_{ri} represents the disturbance and uncertainties; r is the wheel radius.

B. Problem formulation

To synthesize a control law with the dynamics(3),(6), the output redefinition technique is used[42]. The new output equations are defined as

$$\mathbf{z} = \begin{bmatrix} z_x \\ z_y \end{bmatrix} = \begin{bmatrix} x + L\cos(\phi) \\ y + L\sin(\phi) \end{bmatrix} \quad (7)$$

where $L > 0$ is chosen as a constant. Considering the dynamic equation(2) and equation(7), we can obtain a new dynamic formula.

$$\mathbf{M}_t \ddot{\mathbf{z}} + \mathbf{C}_t \dot{\mathbf{z}} = \mathbf{T}\mathbf{u} + \mathbf{d}_t + \tilde{\Delta}_t \quad (8)$$

where $\mathbf{M}_t = \mathbf{TMT}^{-1}$ is the mass matrix; $\mathbf{C}_t = \mathbf{TMT}^{-1}$ represents the Coriolis matrix; $\mathbf{d}_t = \mathbf{Td} + \mathbf{A}_t$, $\mathbf{A}_t = [-m\omega v_y, J/L\dot{v}_y]^T$ represents the lumped disturbances; $\tilde{\Delta}_t = \mathbf{T}\tilde{\Delta}$ is the uncertainties. And \mathbf{T} is defined as

$$\mathbf{T} = \begin{bmatrix} \cos(\phi) & -L\sin(\phi) \\ \sin(\phi) & L\cos(\phi) \end{bmatrix} \quad (9)$$

The equation(8) has the following properties

Property 1. The matrix \mathbf{M}_t is symmetric and positive definite.

Property 2. The matrix $\dot{\mathbf{M}}_t - 2\mathbf{C}_t$ is a skew-symmetric matrix.

From the dynamics(3) and (6), it can be found that the diving forces and torques are resulted from the wheel slip. Thus, differentiating the first equation of (5), we can obtain the wheel slip dynamic model as

$$\begin{aligned} \dot{s}_{xi} &= r_i\dot{\omega}_{ri} - \dot{v}_{xi} \\ &= \frac{r_i}{J_{ri}}(u_{ri} - rF_{xi} - c_{ri}\omega_{ri} - f_{ri} + d_{ri}) - \dot{v}_{xi} \end{aligned} \quad (10)$$

Then, the entire system dynamics from (8)and(10) can be expressed as

$$\begin{aligned}
 (a) \mathbf{M}_t \ddot{\mathbf{z}} &= \mathbf{T}\mathbf{u} - \mathbf{C}_t \dot{\mathbf{z}} + \mathbf{d}_t + \tilde{\Delta}_t \\
 (b) \mathbf{u} &= [u_x, u_\phi]^T, u_x = \sum_{i=1}^4 F_{xi}, u_\phi = \sum_{i=1}^4 M_i \\
 F_{xi} &= N_i \mu S_f(s_i) \frac{s_{xi}}{s_i}, F_{yi} = N_i \mu S_f(s_i) \frac{s_{yi}}{s_i} \\
 (c) \dot{s}_{x1} &= \frac{r_1}{J_{r1}} (u_{r1} - rF_{x1} - c_{r1}\omega_{r1} - A_{f1}S_f(\omega_{r1}) \\
 &\quad + d_{r1}) - \dot{v}_{x1} \\
 &\vdots \\
 \dot{s}_{x4} &= \frac{r_4}{J_{r4}} (u_{r4} - rF_{x4} - c_{r4}\omega_{r4} - A_{f4}S_f(\omega_{r4}) \\
 &\quad + d_{r4}) - \dot{v}_{x4}
 \end{aligned} \quad (11)$$

Define a set of parameters $\theta_t = [\theta_1, \theta_2, \theta_3, \theta_4]^T = [m, J, d_{nx}, d_{ny}]^T$, and the matrices or vectors in (11), namely, \mathbf{M}_t , \mathbf{C}_t , \mathbf{d}_t can be transformed to linear regression form. The wheel dynamics can also be written as linear regression form with the parameters $\theta_{ri} = [\theta_{ri1}, \theta_{ri2}, \dots, \theta_{ri5}]^T = [J_{ri}, c_{ri}, A_{fi}, A_i, d_{ri}]^T$. Generally, the parameter vector θ always varies with working situations such as the change of payloads, thus the actual value can not be exactly known. To design the control law with the parameter uncertainties, we can have the following assumptions[5].

Assumption 1. The lateral slip velocity v_y and its derivative $\|\dot{v}_y\|$ are assumed bounded.

Assumption 2. The extent of the parameters and uncertain nonlinearities are known, i.e.,

$$\theta \in \Omega \triangleq \{\theta : \theta_{min} \leq \theta \leq \theta_{max}\} \quad (12)$$

$$\tilde{\mathbf{d}} \in \triangleq \{\mathbf{d} : |\tilde{\mathbf{d}}| \leq \delta_d\} \quad (13)$$

where $\theta_{min} = [\theta_{1min}, \theta_{2min}, \dots, \theta_{nmin}]^T$, $\theta_{max} = [\theta_{1max}, \theta_{2max}, \dots, \theta_{nmax}]^T$ and δ_d are known.

Remark 1. Note that the above assumptions are reasonable. From the engineering perspective, the lateral velocity is very small compared with mobile robot velocity, and can be assumed bounded in a known range or function. As for the assumption2, though influenced by various aspects(e.g. loads, temperature), the bounds of the parameters(e.g. mass, friction) usually can be decided in advance. Thus, we made these assumptions.

Considering the the entire dynamic model(11), the objective of this paper is to propose a control law of the four-wheel independently driven mobile robot, such that the over-actuated problem, wheel/ground interactions and wheel dynamics can be properly handled and the desired trajectory can be tracked as well.

III. CONTROLLER DESIGN

A. Overall control architecture

Based on the entire dynamic model of the mobile robot(11), our control scheme was proposed to achieve the trajectory tracking task. And it can be found that the primary control

challenges of the mobile robot are follows:1) the over-actuated feature resulted from four independent wheels; 2)the influence from wheel dynamics. To deal with the stated problems, a three-level control architecture consisting of a high-level adaptive robust control, a middle-level control allocation and a low-level wheel slip controller is proposed, as shown in Fig.4.

a) The high-level controller is designed for trajectory tracking. A desired virtual driving force and yaw moments(virtual control law \mathbf{u}_v) is synthesized such that the mobile robot can track the desired trajectory \mathbf{z}_d with $\mathbf{u} = \mathbf{u}_v$.

b) The main purpose of the middle-level controller is to deal with the over-actuated problem. The desired wheel slips s_{xid} are allocated to the low-level with the virtual control law \mathbf{u}_v . The relations between the low-level wheel slip system(11)(c) and high-level robot chasis system(11)(a) is represented by friction formulation.

c) The low-level controller is designed to regulate the wheel slip. With wheel slip reference s_{xid} , the motor torque u_{ri} is calculated such that the wheel slip s_{xi} tracks the desired one.

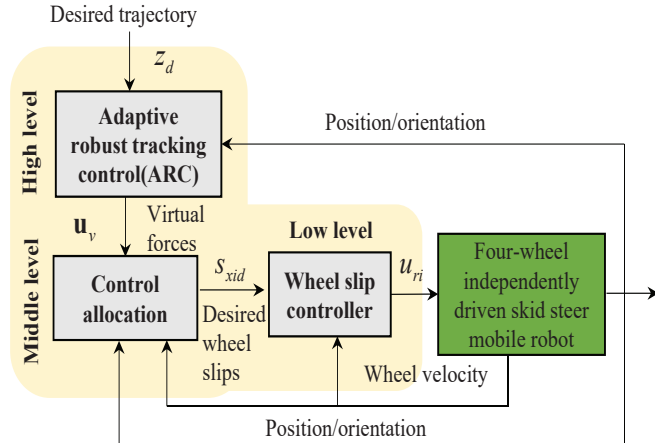


Fig. 4. Overall control architecture

B. The High Level ARC Controller

1) *Discontinuous Projection:* The estimate of parameters θ is defined as $\hat{\theta}$ and the parameter estimation error $\tilde{\theta}$ can be written as $\tilde{\theta} = \hat{\theta} - \theta$. Then, we can have the following adaptation law with discontinuous projection modification[43]

$$\dot{\hat{\theta}} = Proj_{\hat{\theta}}(\Gamma\tau) \quad (14)$$

where Γ is chosen as a diagonal positive matrix and τ is an adaptation function. The projection mapping $Proj_{\hat{\theta}}(\bullet) = [Proj_{\hat{\theta}}(\bullet_1), \dots, Proj_{\hat{\theta}}(\bullet_3)]$ is defined in [43] as

$$Proj_{\hat{\theta}_i}(\bullet_i) = \begin{cases} 0, & \text{if } \hat{\theta}_i = \theta_{imax} \text{ and } \bullet_i > 0 \\ 0, & \text{if } \hat{\theta}_i = \theta_{imin} \text{ and } \bullet_i < 0 \\ \bullet_i, & \text{otherwise} \end{cases} \quad (15)$$

The following conditions are guaranteed with the projection mapping in(15) for any adaptation function τ .

$$\mathbf{P1}) \quad \theta \in \Omega \triangleq \{\theta : \theta_{min} \leq \theta \leq \theta_{max}\} \quad (16)$$

$$\mathbf{P2}) \quad \tilde{\theta}(\Gamma^{-1}Proj_{\hat{\theta}}(\Gamma\tau) - \tau) \leq 0, \forall \tau \quad (17)$$

2) *ARC control algorithm*: Let $\mathbf{e} = \mathbf{z} - \mathbf{z}_d$ be the tracking error, where \mathbf{z}_d is the desired trajectory. Thus, a switching-function-like quantity is defined as

$$\mathbf{p} = \dot{\mathbf{e}} + \Lambda \mathbf{e} \quad (18)$$

where $\Lambda > 0$ is a diagonal matrix used as feedback gain. Thus, we can obtain the error dynamics by differentiating equation(18)

$$\mathbf{M}_t \dot{\mathbf{p}} = \mathbf{T}\mathbf{u} - \mathbf{C}_t \dot{\mathbf{e}} + \mathbf{d}_t + \tilde{\Delta}_t - \mathbf{M}_t \ddot{\mathbf{z}}_d + \mathbf{M}_t \Lambda \dot{\mathbf{e}} \quad (19)$$

Furthermore, the terms in(19) can be written as linear regression form

$$\mathbf{M}_t (\ddot{\mathbf{z}}_d - \Lambda \dot{\mathbf{e}}) + \mathbf{C}_t \dot{\mathbf{z}} - \mathbf{d}_t = -\Psi^T(\mathbf{z}, \dot{\mathbf{z}}, t) \boldsymbol{\theta}_t \quad (20)$$

where $\Psi = [\phi_x, \phi_y] \in R^{4 \times 2}$ is the regressor matrix, $\phi_x = [-(\ddot{z}_{xd} - \Lambda_x e_x) c\varphi^2 - (\ddot{z}_{yd} - \Lambda_y e_y) c\varphi s\varphi + \dot{z}_x \dot{\varphi} c\varphi s\varphi - \dot{z}_y \dot{\varphi} c\varphi^2, -(\ddot{z}_{xd} - \Lambda_x e_x) s\varphi^2 + (\ddot{z}_{yd} - \Lambda_y e_y) c\varphi s\varphi - \dot{z}_x \dot{\varphi} c\varphi s\varphi - \dot{z}_y \dot{\varphi} s\varphi^2, -1, 0]^T$, $\phi_y = [-(\ddot{z}_{xd} - \Lambda_x e_x) c\varphi s\varphi - (\ddot{z}_{yd} - \Lambda_y e_y) s\varphi^2 + \dot{z}_x \dot{\varphi} s\varphi^2 + \dot{z}_y \dot{\varphi} s\varphi c\varphi, (\ddot{z}_{xd} - \Lambda_x e_x) c\varphi s\varphi - (\ddot{z}_{yd} - \Lambda_y e_y) c\varphi^2 + \dot{z}_x \dot{\varphi} c\varphi + \dot{z}_y \dot{\varphi} s\varphi c\varphi, 0, -1]^T$.

Noting the equations(19)(20), we can have the following adaptive robust control law

$$\mathbf{u}_v = \mathbf{T}^{-1}(\mathbf{u}_a + \mathbf{u}_s), \mathbf{u}_a = -\Psi^T(\mathbf{z}, \dot{\mathbf{z}}, t) \hat{\boldsymbol{\theta}}_t \quad (21)$$

where \mathbf{u}_a is the model compensation law, and \mathbf{u}_s is a robust feedback control law. The adaptation function τ_1 is given as

$$\tau_1 = \Psi \mathbf{p} \quad (22)$$

The robust feedback control law \mathbf{u}_s consists of two terms

$$\mathbf{u}_s = \mathbf{u}_{s1} + \mathbf{u}_{s2}, \mathbf{u}_{s1} = -\mathbf{K}\mathbf{p} \quad (23)$$

where \mathbf{u}_{s1} is a proportional feedback law and \mathbf{K} is chosen as a positive and symmetric matrix; \mathbf{u}_{s2} is a feedback part used to guarantee the robust performance with the effect of model uncertainties. With the Assumption 1 and $P1$, there exists a \mathbf{u}_{s2} satisfies the following two conditions

$$\begin{aligned} 1) \quad & \mathbf{p}^T(\mathbf{u}_{s2} - \Psi^T(\mathbf{z}, \dot{\mathbf{z}}, t) \tilde{\boldsymbol{\theta}}_t + \tilde{\Delta}) \leq \epsilon_1 \\ 2) \quad & \mathbf{p}^T \mathbf{u}_{s2} \leq 0 \end{aligned} \quad (24)$$

where ϵ_1 is a design parameter that can be arbitrarily small. Let $\mathbf{p}_2 = \mathbf{u} - \mathbf{u}_v$ denote the input discrepancy. Define positive-definite function V_1 as $V_1 = 1/2 \mathbf{p}^T \mathbf{M}_t \mathbf{p}$, and the differential equation can be derived

$$\dot{V}_1 = \mathbf{p}^T \mathbf{T} \mathbf{p}_2 + \mathbf{p}^T (\mathbf{u}_{s2} - \Psi^T \tilde{\boldsymbol{\theta}}_t + \tilde{\Delta}) - \mathbf{K} \mathbf{p}^T \mathbf{p} \quad (25)$$

C. Middle level control allocation

In high-level controller design, as shown from (25), if $\mathbf{p}_2 = 0$ is satisfied, the trajectory tracking would be achieved with the ARC control law. Therefore, a control law is necessary to be synthesized properly so that the \mathbf{p}_2 will converge to zero or a small value. It should also be noted that, the driving forces for the mobile robot is generated from the interactions between wheel and ground. Thus, the desired wheel slips s_{xid} can be obtained with the virtual driving force and yaw moment(virtual input \mathbf{u}_v). However, compared

with the traditional backstepping controller design, the over-actuated feature should be first attenuated in this paper. Thus, in this section, the control allocation is proposed to obtain the desired wheel slips s_{xid} from the desired virtual input \mathbf{u}_v . Thus, to address the over-actuated problem, an optimization method should be used. The cost function to be optimized is chosen as following to obtain the desired wheel slips with the coupling friction characteristics[44]. Then, we can obtain the cost function as follow.

$$J_{cost} = \sum_{i=1}^4 \frac{F_{xi}^2 + F_{yi}^2}{N_i^2} \quad (26)$$

where N_i represents the vertical force of each wheel. We also have the following constraints

$$u_{xv} = \sum_{i=1}^4 F_{xi} = \sum_{i=1}^4 f_x(s_{xid}), u_{\phi v} = \sum_{i=1}^4 M_i = \sum_{i=1}^4 f_\phi(s_{xid}) \quad (27)$$

Remark 2. Physically, this constraint means that the theoretical combined driving force and torque should be equal to the desired ones.

Referred to the friction model (4), the equation(26) and (27) can be rewritten as

$$J_{cost} = \sum_{i=1}^4 W_i \frac{(A_i \text{atan}(\alpha \sqrt{s_{xid}^2 + s_{yi}^2}))}{N_i^2} \quad (28)$$

$$s.t. \left\{ \begin{array}{l} \sum_{i=1}^n (N_i \mu \text{atan}(\alpha \sqrt{s_{xid}^2 + s_{yi}^2}) \frac{s_{xid}}{\sqrt{s_{xid}^2 + s_{yi}^2}}) = u_{xv} \\ \sum_{i=1}^n (a_i N_i \mu \text{atan}(\alpha \sqrt{s_{xid}^2 + s_{yi}^2}) \frac{s_{xid}}{\sqrt{s_{xid}^2 + s_{yi}^2}} + b_i N_i \mu \text{atan}(\alpha \sqrt{s_{xid}^2 + s_{yi}^2}) \frac{s_{yi}}{\sqrt{s_{xid}^2 + s_{yi}^2}}) = u_{\phi v} \end{array} \right. \quad (29)$$

Thus, the desired wheel slip s_{xid} can be calculated by solving the nonlinear optimization problem with equality constraints. The lagrange multiplier and Newton method are applied to search the optimal solution[44]. Then, we can obtain the following equation

$$\begin{aligned} \dot{V}_1 &= \mathbf{p}^T \mathbf{T} \mathbf{p}_2 + \mathbf{p}^T (\mathbf{u}_{s2} - \Psi^T \tilde{\boldsymbol{\theta}}_t + \tilde{\Delta}) - \mathbf{K} \mathbf{p}^T \mathbf{p} \\ &= \mathbf{p}^T \mathbf{T} \left[\begin{array}{c} \sum_{i=1}^4 (f_x(s_{xi}) - f_x(s_{xid})) \\ \sum_{i=1}^4 (f_\phi(s_{xi}) - f_\phi(s_{xid})) \end{array} \right] \\ &\quad + \mathbf{p}^T (\mathbf{u}_{s2} - \Psi^T \tilde{\boldsymbol{\theta}}_t + \tilde{\Delta}) - \mathbf{K} \mathbf{p}^T \mathbf{p} \end{aligned} \quad (30)$$

According to the mean value theorem, we have that there exist ϵ_{xi} and $\epsilon_{\phi i}$ such that

$$\begin{aligned} f_x(s_{xi}) - f_x(s_{xid}) &= f'_x(\epsilon_{xi})(s_{xi} - s_{xid}) \\ f_\phi(s_{xi}) - f_\phi(s_{xid}) &= f'_\phi(\epsilon_{\phi i})(s_{xi} - s_{xid}) \end{aligned} \quad (31)$$

Then, the equation(30) can be rewritten as

$$\begin{aligned} \dot{V}_1 &= \mathbf{p}^T \mathbf{T} \left[\begin{array}{c} \sum_{i=1}^4 f'_x(\epsilon_{xi})(s_{xi} - s_{xid}) \\ \sum_{i=1}^4 f'_\phi(\epsilon_{\phi i})(s_{xi} - s_{xid}) \end{array} \right] \\ &\quad + \mathbf{p}^T (\mathbf{u}_{s2} - \Psi^T \tilde{\boldsymbol{\theta}}_t + \tilde{\Delta}) - \mathbf{K} \mathbf{p}^T \mathbf{p} \end{aligned} \quad (32)$$

D. Low level Wheel slip

Let $e_{ri} = s_{xi} - s_{xid}$ denote the input discrepancy. As seen from (32), the e_{ri} is expected to be zero. Therefore, the subsection is to synthesize the control inputs such that e_{ri} converges to zero or a small value. From equation(10)

$$\begin{aligned}\dot{e}_r = \frac{r_i}{J_{ri}}(u_{ri} - rF_{xi} + d_{ri} - c_{ri}\omega_{ri} \\ - A_{fi}S_f(\omega_{ri}) - (\dot{v}_{xi} + \dot{s}_{xid})J_{ri}/r)\end{aligned}\quad (33)$$

Then, noticing that we can linearize the term in(33)

$$\begin{aligned}\phi_{ri}^T\theta_{ri} = -(\dot{v}_{xi} + \dot{s}_{xid})/r\theta_{ri1} - \omega_{ri}\theta_{ri2} \\ - S_f(\omega_{ri})\theta_{ri3} - rS_f(s_{xi})\theta_{ri4} + \theta_{ri5}\end{aligned}\quad (34)$$

where the regressor ϕ_{ri} can be defined as

$$\phi_{ri} = [-(\dot{v}_{xi} + \dot{s}_{xid})/r, -\omega_{ri}, -S_f(\omega_{ri}), -rS_f(s_{xi}), 1]^T\quad (35)$$

With the error dynamics (33), to synthesize a control input u_{ri} such that e_{ri} converges to zero or a small value, we define the function V as

$$V = V_1 + 1/2 \sum_{i=1}^n (J_{ri}/re_{ri}^2)\quad (36)$$

Then, we can obtain that

$$\begin{aligned}\dot{V} = \dot{V}_{1|\mathbf{u}_v} + \mathbf{p}^T \mathbf{T} \left[\begin{array}{c} \sum_{i=1}^4 f'_x(\epsilon_{xi})e_{ri} \\ \sum_{i=1}^4 f'_\phi(\epsilon_{\phi_i})e_{ri} \end{array} \right] \\ + \sum_{i=1}^4 e_{ri}(u_{ri} + \phi_{ri}^T\theta_{ri} + \tilde{d}_{ri}) \\ = \dot{V}_{1|\mathbf{u}_v} + \sum_{i=1}^4 e_{ri} \left\{ \mathbf{p}^T \mathbf{T} \left[\begin{array}{c} f'_x(\epsilon_{xi}) \\ f'_\phi(\epsilon_{\phi_i}) \end{array} \right] \right. \\ \left. + u_{ri} + \phi_{ri}^T\theta_{ri} + \tilde{d}_{ri} \right\}\end{aligned}\quad (37)$$

With the equation(37), the ARC control law u_{ri} is proposed as

$$\begin{aligned}u_{ri} &= u_{ria} + u_{ris}, u_{ria} = -\phi_{ri}^T\hat{\theta}_{ri} \\ u_{ris} &= u_{ris1} + u_{ris2}, u_{ris1} = -k_{ris1}e_{ri} \\ \tau_{ri} &= -\phi_{ri}e_{ri}\end{aligned}\quad (38)$$

The u_{ris2} satisfy the following two conditions

$$\begin{aligned}1) \quad e_{ri}(u_{ris2} - \phi_{ri}^T\hat{\theta}_{ri} + \tilde{d}_{ri}) &\leq e_{ri} \\ 2) \quad e_{ri}u_{ris2} &\leq 0\end{aligned}\quad (39)$$

Theorem 1. Considering the system described by(11), the following results can be obtained with the proposed control law.

A) In general, all signals are bounded. Furthermore, the positive definite function $V(t)$ is bounded above by

$$V(t) \leq \exp(-\lambda t)V(0) + \frac{\eta}{\lambda}[1 - \exp(-\lambda t)]\quad (40)$$

where $\lambda = \min\{2\sigma_{\min}(\mathbf{K}\mathbf{M}_t^{-1}), 2k_{ris1}r/J_{ri}, i = 1, 2, 3, 4\}$ and σ_{\min} denotes the minimum eigenvalue of a matrix. $\eta = \epsilon_1 + \sum_{i=1}^4 \epsilon_{ri}$.

B) Suppose after a finite time t_0 , there exist parametric uncertainties only, i.e., $\tilde{d} = 0 \forall t \geq t_0$. Then, zero final tracking error is also achieved.

Proof. The time derivative of the function V defined by is

$$\begin{aligned}\dot{V} &= \mathbf{p}^T \mathbf{T} \mathbf{p}_2 + \mathbf{p}^T (\mathbf{u}_{s2} - \Psi^T \tilde{\theta}_t + \tilde{\Delta}) - \mathbf{K} \mathbf{p}^T \mathbf{p} \\ &\quad + \sum_{i=1}^4 e_{ri}(u_{ri} + \phi_{ri}^T \theta_{ri} + \tilde{d}_{ri}) \\ &= -\mathbf{K} \mathbf{p}^T \mathbf{p} + \epsilon_1 + \sum_{i=1}^4 e_{ri}(-k_{ris1}e_{ri} \\ &\quad + u_{ris2} - \phi_{ri}^T \tilde{\theta}_{ri} + \tilde{d}_{ri}) \\ &\leq -\mathbf{K} \mathbf{p}^T \mathbf{p} + \epsilon_1 - \sum_{i=1}^4 k_{ris1}e_{ri}^2 + \sum_{i=1}^4 \epsilon_{ri} \\ &\leq -\lambda V + \epsilon\end{aligned}\quad (41)$$

which leads to part A of Theorem1 and thus proves of the results.

Now consider the situation in B of Theorem 1,when $\tilde{d} = 0$, $\forall t \geq t_0$. Select a positive definite function V_a as

$$V_a = V(t) + \frac{1}{2}\tilde{\theta}^T \Gamma^{-1} \tilde{\theta} + \frac{1}{2} \sum_{i=1}^4 \tilde{\theta}_{ri}^T \Gamma_{ri}^{-1} \tilde{\theta}_{ri}\quad (42)$$

With condition 2 of the robust performance condition (24)(39) and the property P2 of(17) for the projection type parameter adaptation law, the time derivative of V_a defined by (42) is

$$\begin{aligned}\dot{V}_a &= -\mathbf{K} \mathbf{p}^T \mathbf{p} + \mathbf{p}^T (\mathbf{u}_{s2} - \Psi^T \tilde{\theta}_t) + \tilde{\theta}_t^T \Gamma^{-1} \dot{\tilde{\theta}}_t \\ &\quad + \sum_{i=1}^4 e_{ri}(-k_{ris1}e_{ri} + u_{ris2} - \phi_{ri}^T \tilde{\theta}_{ri}) + \sum_{i=1}^4 \tilde{\theta}_{ri}^T \Gamma_{ri}^{-1} \dot{\tilde{\theta}}_{ri} \\ &\leq -\mathbf{K} \mathbf{p}^T \mathbf{p} - \mathbf{p}^T \Psi^T \tilde{\theta}_t + \tilde{\theta}_t^T \Gamma^{-1} (\text{Proj}(\Gamma \Psi \mathbf{p})) \\ &\quad - \sum_{i=1}^4 k_{ris1}e_{ri}^2 - \sum_{i=1}^4 e_{ri}(\phi_{ri}^T \tilde{\theta}_{ri}) \\ &\quad + \sum_{i=1}^4 \tilde{\theta}_{ri}^T \Gamma_{ri}^{-1} (\text{Proj}(\Gamma_{ri} \phi_{ri} e_{ri})) \\ &\leq -\mathbf{K} \mathbf{p}^T \mathbf{p} - \sum_{i=1}^4 k_{ris1}e_{ri}^2\end{aligned}\quad (43)$$

Part B of Theorem 1 can thus be proved by the above steps. \square

IV. EXPERIMENTAL RESULTS

A. Experiment Setup

The proposed control scheme is implemented on a four-wheel independently driven skid-steer mobile robot as shown in Fig.5. The mobile robot consists of four independent motors, a 36V battery and NI compact-rio. Since the GPS or vision system is not available in the lab, the position and orientation were estimated by dead reckoning method with the odometry and gyroscope sensors[45]. The NI compact-rio is used to process the signals and implement the control law. For the mobile robot in our lab, we can obtain the parameters

for controller design: $b = 0.25m$, $l_f = l_r = 0.2m$, $M = 52kg$, $J = 3.15kgm^2$, $r = 0.16m$. The bounds of parametric vari-

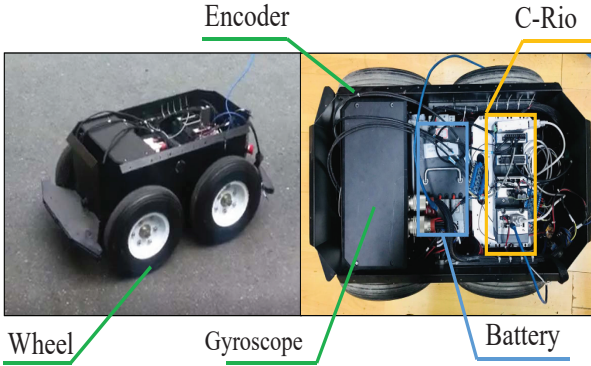


Fig. 5. Skid steer mobile robot

ations are chosen as $\theta_{min} = [50, 2.5, -100, -100]^T$, $\theta_{max} = [78, 5, 100, 100]^T$, $\theta_{rmin} = [0.1, 0.08, 0.05, 0, -1]^T$, $\theta_{rmax} = [0.19, 1, 0.2, 0.5, 1]^T$.

B. Experimental Results

The following control algorithms are implemented and compared.

C1 Kinematic Control Law: To verify the performance of the proposed controller, a traditional kinematic controller with simple motion allocation is compared. From the kinematic equation (1), the desired linear and angular velocities, v_{xd} and ω_d , can be derived by kinematic control law. The parameters of the kinematic controller are set as $K_p = [k_{p1}, k_{p2}]$, $K_d = [k_{d1}, k_{d2}]$ and $K_i = [k_{i1}, k_{i2}]$. Thus, we have the following formula

$$v_d = T\bar{v}, \bar{v} = -K_p e - K_i \int edt - K_d \dot{e} \quad (44)$$

where $v_d = [v_{xd}, \omega_d]^T$ is the desired robot linear and angular velocity. Thus, wheel velocities on each side can be derived with the simple motion allocation

$$\begin{aligned} \omega_{ri} &= (v_{xd} - \omega_d * b)/r, i = 1, 3 \\ \omega_{ri} &= (v_{xd} + \omega_d * b)/r, i = 2, 4 \end{aligned} \quad (45)$$

Let the derived desired wheel velocities in equation(45) be the reference velocity of the driving wheels. This control law gains are properly chosen as $k_{p1} = k_{p2} = 10$, $k_{i1} = k_{i2} = 25$. The desired wheel velocities are tracked by a PID controller, whose gains are properly chosen as $k_i = 56$, $k_p = 4.8$, $k_d = 0$.

C2 Traditional Dynamic Control Law: A traditional dynamic controller for mobile robot is also designed and implemented for comparison, where the wheel driving torques are obtained directly from the high-level ARC controller results u_x and u_ϕ with simple torque allocation. Referred to the research[42], we have the following torque allocation formulas

$$\begin{aligned} \tau_{ri} &= (u_x - u_\phi * b)/2r, i = 1, 3 \\ \tau_{ri} &= (u_x + u_\phi * b)/2r, i = 2, 4 \end{aligned} \quad (46)$$

C3 Proposed Control three-level adaptive robust Law: The Λ is chosen as $\Lambda = diag[5, 5]$. As for the robust control term, the control law is designed as $\mathbf{u}_s = -\mathbf{K}_2 \mathbf{p}$ in the experiments,

where \mathbf{K}_2 represents the combination of \mathbf{u}_{s1} and \mathbf{u}_{s2} [35], which are chosen as $\mathbf{K}_2 = [500, 100]^T$. The adaptation parameters $\mathbf{\Gamma}$ can be set as $\mathbf{\Gamma} = diag[0, 0, 0, 0, 0, 1000, 200, 0, 0]$. For the wheel slip controller, the feedback parameters and adaptation parameters are chosen as $k_{ri} = 4.8, i = 1, 2, 3, 4$, $\mathbf{\Gamma} = diag[0, 0, 0, 0, 56]$.

The following two test sets are used to illustrate the effectiveness of the proposed approach. Since the influence from the ground condition is inevitable, in an effort to make sure the comparison of these controllers are fair, the experiments are carried out on the same ground.

Set 1: The tracking performance is tested with a elliptical trajectory for the controllers.

$$\mathbf{z}_d = \begin{bmatrix} x_d \\ y_d \end{bmatrix} = \begin{bmatrix} 0.4 * \cos(0.1t - \pi/2) \\ 0.5 * \sin(0.1t - \pi/2) + 0.5 \end{bmatrix} \quad (47)$$

Set 2: The tracking performance is tested with a 8-type trajectory.

$$\mathbf{z}_d = \begin{bmatrix} x_d \\ y_d \end{bmatrix} = \begin{bmatrix} 0.5 * \cos(0.1t - \pi/2) \\ 0.5 * \sin(0.05t - \pi/2) + 0.5 \end{bmatrix} \quad (48)$$

The following indices will be used to quantify the performance for comparisons[46]:

1) $\|e_x\|_{rms}$, $\|e_y\|_{rms}$, the root-mean-square value of the tracking error, is used measure the tracking performance.

2) $\|e_x\|_{max}$, $\|e_y\|_{max}$, the maximum absolute value of the tracking error is used measure the tracking performance.

3) $\|\omega_{ri}\|_{max}$, the maximum wheel velocity is to measure the wheel performance.

For Set1, the desired trajectory tracking performance are presented in Fig.6, demonstrating that the proposed controller can work well for trajectory tracking task. The experimental tracking error are shown in Fig.7, and the root-mean-square-error value of the tracking error $\|e_x\|_2$, $\|e_y\|_2$, are used to measure the average tracking performance. The indexes for the controllers are shown in Table.I. From the tracking error results, we can conclude that the proposed controller C3 performances better than the traditional controller C1 and C2. The wheel velocities are presented in Fig.8 and Table.II, with the elliptical trajectory tracking for different controllers. From the figure, we can find out that, the wheel velocities on the same side are similar with the controller C1 and C3, while the wheel velocities of C2 various with each other. For C1, it is seen from the simple motion allocation(45) that the desired wheel velocities are assumed same with each other, which are tracked by a PID controller. Compared with C1, the proposed low-level controller is designed to track the desired wheel slip. Since the wheel slips on each side are assumed same, thus, the wheel velocities for both controller are similar. As for C2, we found the unexpected phenomenon that the wheel velocities varies much different with each other, one of which may become very large. It is resulted from that the driving torque is allocated directly, where the input torques are equals to each other on the same side, while motor frictions and wheel/ground interactions are usually different from each other(e.g. one of wheels may lift from ground).

Furthermore, an experiment for 8-type trajectory tracking is compared. From the trajectory tracking performance as shown

TABLE I
PERFORMANCE INDEX, SET1

Algorithms	$\ e_x\ _2$	$\ e_x\ _{max}$	$\ e_y\ _2$	$\ e_y\ _{max}$
C1	2.47e-4	3.7e-3	1.00e-4	2.40e-4
C2	1.15e-4	1.4e-3	1.06e-4	3.47e-4
C3	8.61e-5	1.2e-3	5.84e-5	2.40e-4

TABLE II
WHEEL VELOCITY INDEX, SET1

Algorithms	$\ \omega_{r1}\ _{max}$	$\ \omega_{r2}\ _{max}$	$\ \omega_{r3}\ _{max}$	$\ \omega_{r4}\ _{max}$
C1	1.14	0.17	1.11	0.15
C2	0.76	0.54	2.34	0.60
C3	1.06	0.20	1.14	0.17

in Fig.9, acceptable performances are presented for the controllers . Though the 8-type trajectory is much complex than elliptical contouring, the proposed controller C3 still achieve a better performance from Fig.10 and the quantitative performance indexes Table.III. The wheel velocity performance is presented in Fig.11 and Table.IV. The above experimental results demonstrate that the proposed three-level controller can not only achieve a good trajectory tracking performance but also deal with the over-actuated problem, wheel/ground interactions and wheel dynamics simultaneously.

TABLE III
PERFORMANCE INDEX, SET2

Algorithms	$\ e_x\ _2$	$\ e_x\ _{max}$	$\ e_y\ _2$	$\ e_y\ _{max}$
C1	4.09e-4	4.4e-3	2.17e-4	5.45e-4
C2	2.11e-4	1.8e-3	2.21e-4	6.82e-4
C3	1.42e-4	1.4e-3	2.13e-4	5.29e-4

TABLE IV
WHEEL VELOCITY INDEX, SET2

Algorithms	$\ \omega_{r1}\ _{max}$	$\ \omega_{r2}\ _{max}$	$\ \omega_{r3}\ _{max}$	$\ \omega_{r4}\ _{max}$
C1	0.80	0.83	0.81	0.84
C2	0.81	0.80	2.67	1.60
C3	0.81	0.82	0.82	0.81

V. CONCLUSION

In this paper, an integrated dynamical model for the four-wheel independently driven mobile robots is firstly developed including chassis kinematics, chassis dynamics, wheel/ground interactions, and wheel dynamics. A model-based coordinated adaptive robust control scheme is proposed with the dynamic model. Compared with the tradition controller, the proposed controller directly generates the motor driving torque commands for four wheels with a three-level overall control architecture. In the high level, by mainly focusing on the chassis dynamics, an adaptive robust control law is proposed to track the desired robot motion trajectory and generates virtual friction driving force for the later middle level control design. In the middle level, a control allocation technique is applied to deal with the over-actuated feature such that the wheel slip reference is calculated for each wheel in the low-level design. And in the low level, the wheel slip control is

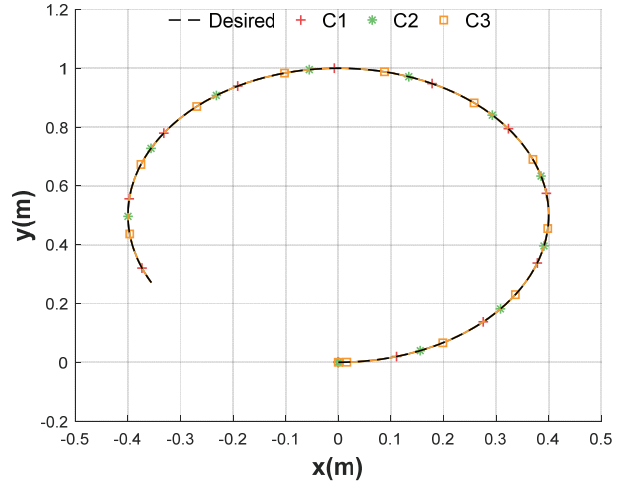


Fig. 6. Elliptical trajectory tracking performance

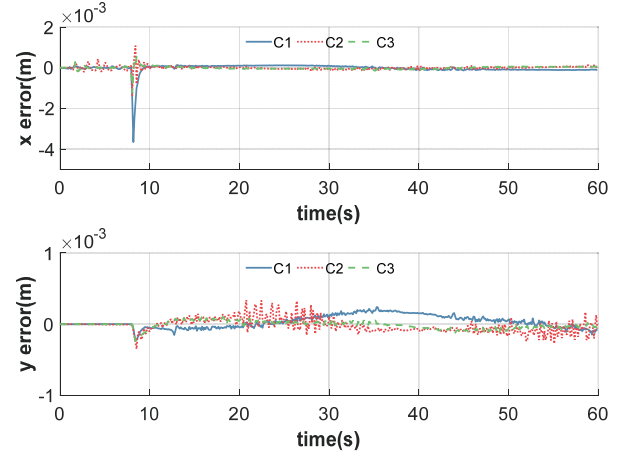


Fig. 7. Tracking error of of Set 1: a) axis x; b)axis y

designed to track the desired slip reference by considering the wheel dynamics. The stability and tracking performance of this three-level adaptive robust control scheme are theoretically guaranteed. Comparative experiments with traditional methods are carried out, and the experimental results show the better performance of our proposed scheme.

REFERENCES

- [1] E. Mohammadpour and M. Naraghi, "Robust adaptive stabilization of skid steer wheeled mobile robots considering slipping effects," *Advanced Robotics*, vol. 25, no. 1-2, pp. 205–227, 2011.
- [2] C. J. Ostafew, A. P. Schoellig, and T. D. Barfoot, "Robust constrained learning-based nmpc enabling reliable mobile robot path tracking," *The International Journal of Robotics Research*, vol. 35, no. 13, pp. 1547–1563, 2016.
- [3] Z.-G. Hou, A.-M. Zou, L. Cheng, and M. Tan, "Adaptive control of an electrically driven nonholonomic mobile robot via backstepping and fuzzy approach," *IEEE Transactions on Control Systems Technology*, vol. 17, no. 4, pp. 803–815, 2009.
- [4] J. Huang, C. Wen, W. Wang, and Z.-P. Jiang, "Adaptive output feedback tracking control of a nonholonomic mobile robot," *Automatica*, vol. 50, no. 3, pp. 821–831, 2014.
- [5] J. C. Ryu and S. K. Agrawal, "Differential flatness-based robust control of mobile robots in the presence of slip," *International Journal of Robotics Research*, vol. 30, no. 4, pp. 463–475, 2011.

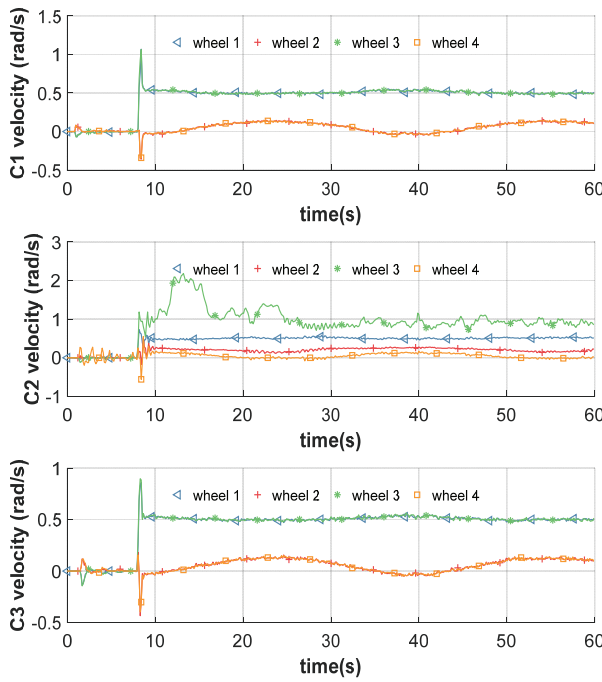


Fig. 8. Wheel velocities of Set 1

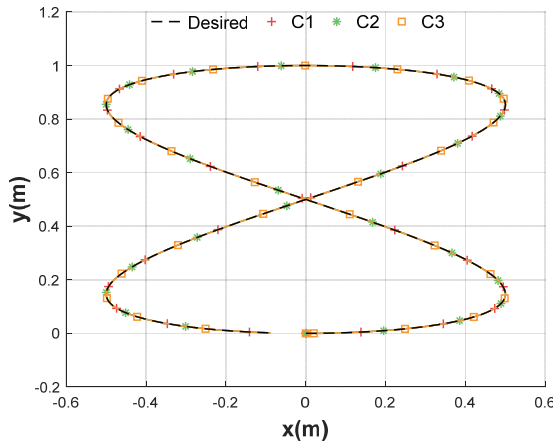


Fig. 9. 8-type trajectory tracking performance

- [6] W. Sun, S. Tang, H. Gao, and J. Zhao, "Two time-scale tracking control of nonholonomic wheeled mobile robots," *IEEE Transactions on Control Systems Technology*, vol. 24, no. 6, pp. 2059–2069, 2016.
- [7] B. L. Chang and D. Wang, "Gps-based tracking control for a car-like wheeled mobile robot with skidding and slipping," *Mechatronics IEEE/ASME Transactions on*, vol. 13, no. 4, pp. 480–484, 2008.
- [8] C. B. Low and D. Wang, "Gps-based path following control for a car-like wheeled mobile robot with skidding and slipping," *IEEE Transactions on Control Systems Technology*, vol. 16, no. 2, pp. 340–347, 2008.
- [9] Z. Li, J. Deng, R. Lu, and Y. Xu, "Trajectory-tracking control of mobile robot systems incorporating neural-dynamic optimized model predictive approach," *IEEE Transactions on Systems, Man, And cybernetics:systems*, vol. 46, no. 6, pp. 740–749, 2016.
- [10] A. Mazur and M. Cholewski, "Virtual force concept in steering mobile manipulators with skid-steering platform moving in unknown environment," *Journal of Intelligent and Robotic Systems*, vol. 77, no. 3-4, pp. 433–443, 2015.
- [11] O. Elshazly, A. Abo-Ismail, H. S. Abbas, and Z. Zyada, "Skid steering mobile robot modeling and control," in *Control (CONTROL), 2014 UKACC International Conference on*. IEEE, Conference Proceedings, pp. 62–67.
- [12] Y. Chen and J. Wang, "Adaptive energy-efficient control allocation for planar motion control of over-actuated electric ground vehicles," *Control Systems Technology, IEEE Transactions on*, vol. 22, no. 4, pp. 1362–1373, 2014.
- [13] ———, "Design and experimental evaluations on energy efficient control allocation methods for overactuated electric vehicles: Longitudinal motion case," *IEEE/ASME Transactions on Mechatronics*, vol. 19, no. 2, pp. 538–548, 2014.
- [14] J. Liao, Z. Chen, and B. Yao, "Performance-oriented coordinated adaptive robust control for four-wheel independently driven skid steer mobile robot," *IEEE Access*, vol. PP, no. 99, pp. 1–1, 2017.
- [15] J. Kang, W. Kim, J. Lee, and K. Yi, "Skid steering-based control of a robotic vehicle with six in-wheel drives," *Proceedings of the Institution of Mechanical Engineers, Part D: Journal of Automobile Engineering*, vol. 224, no. 11, pp. 1369–1391, 2010.
- [16] H. Gao, X. Song, D. Liang, K. Xia, N. Li, and Z. Deng, "Adaptive motion control of wheeled mobile robot with unknown slippage," *International Journal of Control*, vol. 87, no. 8, pp. 1513–1522, 2014.
- [17] W. Sun, Y. Zhang, Y. Huang, H. Gao, and O. Kaynak, "Transient-performance-guaranteed robust adaptive control and its application to precision motion control systems," *IEEE Transactions on Industrial Electronics*, vol. 63, no. 10, pp. 6510–6518, 2016.

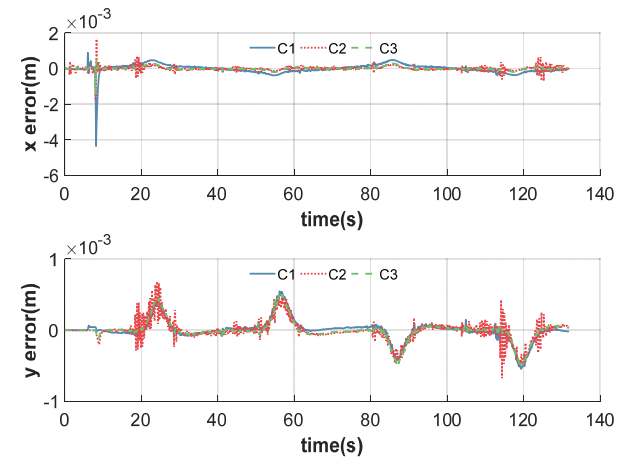


Fig. 10. Tracking error of Set 2: a) axis x ; b) axis y

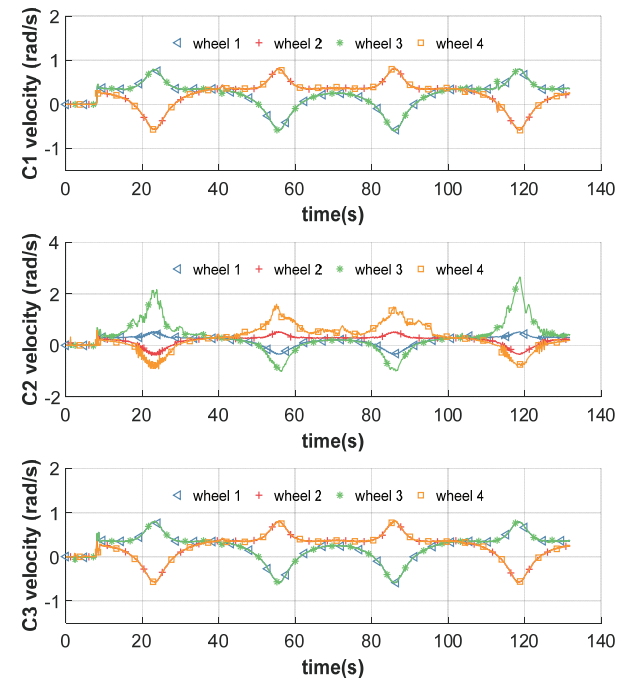
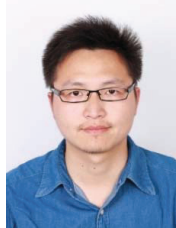


Fig. 11. Wheel velocities of Set 2

- [18] W. Sun, H. Pan, and H. Gao, "Filter-based adaptive vibration control for active vehicle suspensions with electrohydraulic actuators," *IEEE Transactions on Vehicular Technology*, vol. 65, no. 6, pp. 4619–4626, 2016.
- [19] M. Morawiec, "The adaptive backstepping control of permanent magnet synchronous motor supplied by current source inverter," *IEEE Transactions on Industrial Informatics*, vol. 9, no. 2, pp. 1047–1055, 2013.
- [20] J. Yao and W. Deng, "Active disturbance rejection adaptive control of hydraulic servo systems," *IEEE Trans. Ind. Electron*, vol. 64, no. 10, pp. 8023–8032, 2017.
- [21] J. Yao, W. Deng, and Z. Jiao, "Rise-based adaptive control of hydraulic systems with asymptotic tracking," *IEEE Transactions on Automation Science and Engineering*, vol. 14, no. 3, pp. 1524–1531, 2017.
- [22] X. Li, S.-L. Chen, C. S. Teo, and K. K. Tan, "Data-based tuning of reduced-order inverse model in both disturbance observer and feedforward with application to tray indexing," *IEEE Transactions on Industrial Electronics*, 2017.
- [23] J. Ma, S. L. Chen, N. Kamaldin, C. S. Teo, A. Tay, A. A. Mamun, and K. K. Tan, "Integrated mechatronic design in the flexure-linked dual-drive gantry by constrained linear quadratic optimization," *IEEE Transactions on Industrial Electronics*, vol. 65, no. 3, pp. 2408–2418, March 2018.
- [24] Z. Feng and W. X. Zheng, "On extended dissipativity of discrete-time neural networks with time delay," *IEEE Transactions on Neural Networks & Learning Systems*, vol. 26, no. 12, pp. 3293–3300, 2015.
- [25] M. Preindl and S. Bolognani, "Model predictive direct torque control with finite control set for pmsm drive systems, part 2: Field weakening operation," *IEEE Transactions on Industrial Informatics*, vol. 9, no. 2, pp. 648–657, 2013.
- [26] S.-L. Chen, X. Li, C. S. Teo, and K. K. Tan, "Composite jerk feedforward and disturbance observer for robust tracking of flexible systems," *Automatica*, vol. 80, pp. 253–260, 2017.
- [27] A. Sabanovic, "Variable structure systems with sliding modes in motion control—a survey," *IEEE Transactions on Industrial Informatics*, vol. 7, no. 2, pp. 212–223, 2011.
- [28] R. Wang, H. Jing, H. R. Karimi, and N. Chen, "Robust fault-tolerant h_∞ control of active suspension systems with finite-frequency constraint," *Mechanical Systems & Signal Processing*, vol. 62–63, no. 4702, pp. 341–355, 2015.
- [29] S. K. Kommuri, M. Defoort, H. R. Karimi, and K. C. Veluvolu, "A robust observer-based sensor fault-tolerant control for pmsm in electric vehicles," *IEEE Transactions on Industrial Electronics*, vol. 63, no. 12, pp. 7671–7681, 2016.
- [30] T. J. Teo, H. Zhu, S.-L. Chen, G. Yang, and C. K. Pang, "Principle and modeling of a novel moving coil linear-rotary electromagnetic actuator," *IEEE Transactions on Industrial Electronics*, vol. 63, no. 11, pp. 6930–6940, 2016.
- [31] C. Hu, Z. Wang, Y. Zhu, M. Zhang, and H. Liu, "Performance-oriented precision larc tracking motion control of a magnetically levitated planar motor with comparative experiments," *IEEE Transactions on Industrial Electronics*, vol. 63, no. 9, pp. 5763–5773, 2016.
- [32] M. Yuan, Z. Chen, B. Yao, and X. Zhu, "Time optimal contouring control of industrial biaxial gantry: A highly efficient analytical solution of trajectory planning," *IEEE/ASME Transactions on Mechatronics*, vol. 22, no. 1, pp. 247–257, 2017.
- [33] C. Yang, Y. Jiang, Z. Li, W. He, and C.-Y. Su, "Neural control of bimanual robots with guaranteed global stability and motion precision," *IEEE Transactions on Industrial Informatics*, 2017.
- [34] W. He, Y. Ouyang, and J. Hong, "Vibration control of a flexible robotic manipulator in the presence of input deadzone," *IEEE Transactions on Industrial Informatics*, vol. 13, no. 1, pp. 48–59, 2017.
- [35] Z. Chen, Y. Pan, and J. Gu, "Integrated adaptive robust control for multilateral teleoperation systems under arbitrary time delays," *International Journal of Robust & Nonlinear Control*, vol. 26, no. 12, pp. 2708–2728, 2016.
- [36] C. Li, C. Li, Z. Chen, and B. Yao, "Advanced synchronization control of a dual-linear-motor-driven gantry with rotational dynamics," *IEEE Transactions on Industrial Electronics*, vol. 65, no. 9, pp. 7526–7535, 2018.
- [37] Z. Chen, B. Yao, and Q. Wang, " μ -synthesis-based adaptive robust control of linear motor driven stages with high-frequency dynamics: A case study," *IEEE/ASME Transactions on Mechatronics*, vol. 20, no. 3, pp. 1482–1490, 2015.
- [38] ———, "Accurate motion control of linear motors with adaptive robust compensation of nonlinear electromagnetic field effect," *IEEE/ASME Transactions on Mechatronics*, vol. 18, no. 3, pp. 1122–1129, 2013.
- [39] T. A. Johansen and T. I. Fossen, "Control allocation—a survey," *Automatica*, vol. 49, no. 5, pp. 1087–1103, 2013.
- [40] H. Alwi and C. Edwards, "Fault tolerant control using sliding modes with on-line control allocation," *Automatica*, vol. 44, no. 7, pp. 1859–1866, 2008.
- [41] M. G. Feemster and J. M. Esposito, "Comprehensive framework for tracking control and thrust allocation for a highly overactuated autonomous surface vessel," *Journal of Field Robotics*, vol. 28, no. 1, pp. 80–100, 2011.
- [42] E. J. Rodriguez-Seda, C. Tang, M. W. Spong, Stipanović, Du, and M. An, "Trajectory tracking with collision avoidance for nonholonomic vehicles with acceleration constraints and limited sensing," *International Journal of Robotics Research*, vol. 33, no. 12, pp. 1569–1592, 2014.
- [43] B. Yao and M. Tomizuka, "Adaptive robust control of siso nonlinear systems in a semi-strict feedback form," *Automatica*, vol. 33, no. 5, pp. 893–900, 1997.
- [44] O. Mokhiamar and M. Abe, "Simultaneous optimal distribution of lateral and longitudinal tire forces for the model following control," *Journal of Dynamic Systems Measurement & Control*, vol. 126, no. 4, pp. 753–763, 2004.
- [45] H. Chung, L. Ojeda, and J. Borenstein, "Accurate mobile robot dead-reckoning with a precision-calibrated fiber-optic gyroscope," *Robotics & Automation IEEE Transactions on*, vol. 17, no. 1, pp. 80–84, 2001.
- [46] R. Wang, H. Jing, F. Yan, H. R. Karimi, and N. Chen, "Optimization and finite-frequency h_∞ control of active suspensions in in-wheel motor driven electric ground vehicles," *Journal of the Franklin Institute*, vol. 352, no. 2, pp. 468–484, 2015.

Jianfeng Liao received the B.Eng. degree in mechatronic control engineering in 2013 from Zhejiang University, Hangzhou, China, where he is currently working toward the Ph.D. degree in mechatronic control engineering.



Zheng Chen (S'11-M'13-SM'18) received the B.Eng. and Ph.D. degrees in mechatronic control engineering from Zhejiang University, Zhejiang, China, in 2007 and 2012, respectively. From 2013 to 2015, he was a Postdoctoral Researcher in the Department of Mechanical Engineering at Dalhousie University, Halifax, NS, Canada. Since 2015, he has been an associated professor with the Ocean College of Zhejiang University. His research interests mainly focus on advanced control of robotic and mechatronic system (e.g., nonlinear adaptive robust control, motion control, trajectory planning, tele-robotics, exoskeleton, mobile manipulator, precision mechatronic system, underwater robot).



Bin Yao (S'92-M'96-SM'09) received his Ph.D. degree in Mechanical Engineering from the University of California at Berkeley in 1996 after obtaining M.Eng. degree in Electrical Engineering from Nanyang Technological University of Singapore in 1992 and B.Eng. in Applied Mechanics from Beijing University of Aeronautics and Astronautics of China in 1987. He has been with the School of Mechanical Engineering at Purdue University since 1996 and was promoted to the rank of Professor in 2007. He was honored as a Kuang-piu Professor in 2005

and a Changjiang Chair Professor at Zhejiang University by the Ministry of Education of China in 2010 as well. More detailed information can be found at <https://engineering.purdue.edu/~byao>.

